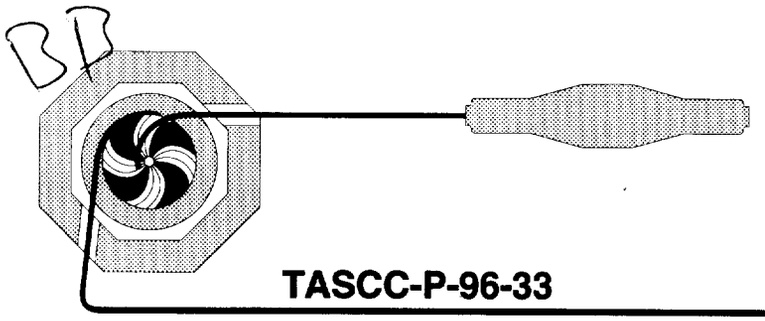

PREPRINT

tascc

TASCC-P-96-33

BETA DECAYS OF ^{44}V AND ^{52}Co

E. Hagberg, I.S. Towner, J.C. Hardy, V.T. Koslowsky and G. Savard
AECL, Chalk River Laboratories, Chalk River, ON K0J 1J0, Canada

S. Sterbenz
Los Alamos National Laboratory, P.O. Box 1663, Los Alamos, N.M. 87545, U.S.A.

Submitted to
Nucl. Phys. A

Physical and Environmental Sciences
Chalk River Laboratories
Chalk River, ON K0J 1J0 Canada

1996 September

Beta Decays of ^{44}V and ^{52}Co

E. Hagberg[a], I.S. Towner[a], J.C. Hardy[a], V.T. Koslowsky[a], G. Savard[a] and S. Sterbenz[b]

a AECL, Chalk River Laboratories, Chalk River, Ontario, Canada K0J 1J0

b Los Alamos National Laboratory, P.O. Box 1663, Los Alamos, N.M. 87545, USA

Abstract

We have studied the previously unknown β^+ decay branches from $^{44,44m}V$ and ^{52}Co to particle-bound states in ^{44}Ti and ^{52}Fe respectively. These intense branches populate a few states in the daughters from an excitation energy of about 1 MeV up to the isobaric analogue states at about 6 MeV. We have measured the first precise energy values for the latter states as well as the β branching ratios to all states in this excitation energy region. We have calculated the β^+ decay of $^{44,44m}V$ in the full fp shell model space as well as in a truncated space. Renormalized transition operators are constructed for the truncated space and tested against experimental data in ^{44}V and ^{52}Co. In general there is good agreement between theory and experiment for the half-lives, level energies and beta branches, but not all the states found are reproduced by the calculations.

PACS codes 21.60.Cs, 23.40.Hc, 27.40 +z

Keywords: Radioactivity $^{44,44m}V$, ^{52}Co; measured E_γ, I_γ, $T_{1/2}$; deduced level energies, branching ratios, ft values; HPGe detectors, plastic scintillators; $\gamma\beta\beta$ and $\gamma\gamma\beta$ coincidences.

email: HAGBERG@CU50.CRL.AECL.CA

1. INTRODUCTION

Neutron-deficient nuclides in the $f_{7/2}$ shell can be divided into three categories according to what is known about them. Those that are close to the valley of β-stability decay by β-delayed γ rays while those that are further away from stability are only known by their β-delayed particle decays. In only a few cases have both decay modes been seen from the same nuclide. The third category comprises nuclides very close to the proton drip-line that are known to be bound, but no decay data have yet been measured.

Together with ^{48}Mn, ^{44}V and ^{52}Co form a series of T_z = -1, odd-odd nuclides within the $f_{7/2}$ proton and neutron shells. Two of them, ^{44}V and ^{48}Mn, are known to decay by β-delayed particle emission, but that decay mode is very weak. Much stronger β-decay branches to particle-bound states at lower excitation energies are expected, including a strong superallowed transition, but they have only been reported for ^{48}Mn[1].

The ^{44}V nuclide was first identified[2] through the observation of about 100 β-delayed alpha particles, which were tentatively assigned to originate from a single state at 8.17 MeV excitation energy in the β-decay daughter ^{44}Ti. Preliminary results of our present work on the β-delayed γ rays from ^{44}V and ^{44m}V have been presented at three conferences[3]. Some of our results have subsequently been confirmed in a study at GANIL by Keller *et al.*[4], aimed at measuring the ratio of isomer to ground state production of ^{42}Sc and ^{44}V in high-energy heavy-ion reactions.

The ^{52}Co isotope was first seen in experiments at GANIL and confirmed to be stable against ground state particle decay[5] but no decay information was obtained. The decay of ^{52}Co was later investigated with the CARP separator and two extremely weak γ rays were tentatively assigned to this nuclide[6]. A half-life value was also obtained from counting high energy positrons. We have reported our preliminary ^{52}Co data at three conferences[3].

There have been several recent studies of Gamow-Teller β decays in light nuclides[7,8] since they offer the possibility of obtaining information on the behavior of the axial-vector current in the nuclear medium, in particular whether the GT strength found by experiment is smaller than that predicted by theory. The most informative test cases are those nuclides that have very high ground state Q_{EC} values so that a large portion of the GT strength function can be explored, including part of the GT resonance. This usually requires a combination of data on β-delayed particle decay (low Q_{EC} values) with those on β-delayed γ rays (high Q_{EC} values). The structure of the explored nuclides should also be sufficiently simple that a shell-model description is accurate.

The $T_z = -1$ isotopes in the $f_{7/2}$ shell fulfill these requirements. Their decay energies are about 14 MeV and they are amenable to shell-model calculations. The GT decays of ^{44}V[9] and ^{48}Mn[1,10] have already been calculated. Furthermore, one might expect some similarities between the treatments of ^{44}V (4 particles in the $f_{7/2}$ shell) and ^{52}Co (4 holes in the same shell).

2. EXPERIMENTAL SETUP

The experiment was performed at the TASCC facility of the Chalk River Laboratories. The activities were produced with $^{40}Ca(^{6}Li, 2n)^{44}V$ and $^{40}Ca(^{14}N, 2n)^{52}Co$ reactions on a stack of natural Ca targets. The energies of the ^{6}Li and ^{14}N beams were 35 MeV and 62 MeV, respectively, and the intensities were typically 200 pnA. A helium-jet transport system with NaCl aerosol was used to thermalize the recoiling reaction products and convey them to a low-background counting location. There, the activity-laden NaCl aerosol clusters were deposited on an aluminized tape and the collected samples periodically moved to a detector station. The sample collection time was controlled by the removal and insertion of a paddle between the helium-jet nozzle and the tape as well as by a second paddle that blocked the heavy-ion beam. The collection time, which equaled the detector counting time, was 500 ms for the ^{44}V experiments and 300 ms for the ^{52}Co experiments. The transportation time in the helium-jet capillary was about 80 ms and the tape transport time to the detector was 100 ms.

Decay data were obtained with two different arrangements. In the first one a 68% efficient HPGe detector was placed at the counting location together with two plastic scintillators, one on either side of the tape. The purpose of this setup was to detect weak γ-ray branches by removing most room background and β^+ induced radiation. This was achieved by the requirement that an event in the HPGe detector was coincident with a positron detected in the scintillator positioned on the other side of the sample from the HPGe and was not coincident with positrons detected in the scintillator positioned on the same side as the HPGe. Five parameters were written on magnetic tape for each event:

the γ-ray energy, the time differences between the γ ray and the positrons in the two scintillators, the time elapsed since counting began on this sample, and the sample number. The setup reported so far has been described in greater detail in a recent publication[11].

The second detector arrangement employed two HPGe detectors, the 68% one and a 40% one, as well as one plastic scintillator at the counting location. All three detectors viewed the sample from different angles, with no overlap in solid angle. This arrangement was used to observe γ-γ coincidences as well as β-γ-γ coincidences.

In a separate experiment, ^{44}V samples were also produced by the Chalk River on-line isotope separator (ISOL)[12]. For this case the helium-jet capillary was connected to the separator helium-jet ion source[13]. The delivered, radioactive nuclei were ionized, accelerated to 40 keV energy, mass analyzed by the ISOL main magnet and then implanted into the aluminized mylar tape of the tape transport station. The detector arrangement was the same γββ one as used in the first method. Only ^{44}V was produced in sufficient quantities to permit an ISOL study.

The energy calibrations of the HPGe detectors used in the gas-jet experiments were achieved with precisely known γ rays originating from known activities present in the collected samples. For the ^{44}V experiments, these activities were ^{20}F, ^{38}K, ^{42m}Sc and ^{43}Ti, whereas for the ^{52}Co experiments they were ^{20}F, ^{42m}Sc, ^{50m,52m}Mn and ^{52}Fe. For the ISOL experiment, the HPGe detector was energy calibrated with standard sources of ^{54}Mn, ^{56,60}Co, ^{88}Y, ^{137}Cs and ^{228}Th, and those sources were also used for all HPGe detector efficiency calibrations.

3. EXPERIMENTAL RESULTS

3.1 ^{44}V and ^{44m}V

Three γ-ray spectra, obtained in our studies on the decay of ^{44}V (and its isomer) are shown in Fig. 1. The majority of events seen in Fig. 1a, obtained with our first experimental arrangement (He-jet, $\gamma\beta\overline{\beta}$), are from ^{44}V. Other activities are also seen and, among them, ^{43}Ti, ^{42m}Sc, ^{44}Sc and ^{38}K originate from reactions of the ^{6}Li beam with the Ca targets whereas ^{28}P and ^{20}F are produced from a small Mg contamination of the targets as well as a Si contaminant introduced in the target-making process. The second most intense activity, ^{43}Ti, has a complicated decay scheme with many γ rays. Fortunately, it has been thoroughly investigated by Honkanen *et al.*[14]. The major γ rays from ^{44}V are seen clearly in Fig. 1b, obtained with the on-line isotope separator ($\gamma\beta\overline{\beta}$), where all other activities except ^{44}Sc, which has the same mass, have been removed. Fig. 1c shows a spectrum obtained from our γ-γ coincidence experiment (He-jet) with a gate on the 1083 keV γ ray, common to ^{44}V and ^{44m}V, and this also shows clearly the strong gamma rays from both decays.

We can unambiguously assign five strong γ rays to the decays of ^{44}V (see Table 1) because of the combination of their presence in our mass-44 ISOL data (Fig. 1b) and their short half-life. The only other candidate nuclides accessible with our beam-target combination, ^{44}Ti and ^{44}Sc, are long-lived. We have also assigned two additional γ rays (2046 and 3032 keV) to vanadium because of their coincidence relationship with the 1083 keV γ ray, although the 3032 keV γ ray only exhibits a tentative coincidence.

Furthermore, although no β-delayed γ rays from ^{44}V were known previous to these experiments, a large number of excited states in the daughter, ^{44}Ti, have been observed in reaction studies and their excitation energies, spins and parities are well known[15]. There is good agreement between the differences in known excitation energies of states in ^{44}Ti and the seven γ rays so far assigned to the decay of ^{44}V. We assign an additional four γ rays to the decays of ^{44}V based solely on their apparent half-life and good agreement with energy differences of ^{44}Ti states. The γ ray at 2948 keV is tentatively assigned to ^{44}V based on its apparent half-life and the fact that its energy does not agree with known γ rays from any other identified activity produced in our experiments.

Our results for the γ rays we have assigned to the decays of ^{44}V are shown in Table 1. A perusal of the half-lives measured for each γ ray reveals that they are clustered in two groups, one centered around a value of 111 ms and the other one centered around 150 ms. Furthermore, the γ-γ coincidence data also show two distinct patterns with the γ rays associated with the same pattern having similar half-lives. The most intense γ ray assigned to ^{44}V, at 1083 keV, is common to both groups and exhibits an intermediate half-life.

The mirror nuclide of ^{44}V, ^{44}Sc, is known to have a 2^+ ground state and a 6^+ isomeric state at an excitation energy of 271 keV[15]. A similar structure is thus expected in ^{44}V. A 6^+ isomeric state in ^{44}V would β decay predominantly by a superallowed transition to its 6^+, T=1 isobaric analogue state in ^{44}Ti and then be followed by a γ ray cascade through lower-lying 4^+ and 2^+ states in the even-even ^{44}Ti nuclide. Such a decay

pattern is indeed seen for those γ rays exhibiting the 150 ms half-life. We assign them to the decay of an isomeric 6^+ state in ^{44}V.

Our proposed decay scheme for ^{44m}V is shown in Fig. 2. The excitation energies deduced from our work, and shown in Table 2, are in good agreement with the data compiled by Endt[15]. The lowest 6^+, T=1 state in ^{44}Ti was not known previously: the superallowed nature of the β transition feeding this state is clearly evident in Table 2. A weak β feeding of the lowest 4^+ state is deduced from our data (6.0±5.1%), but it is practically compatible with zero (as would be expected for a $6^+ \rightarrow 4^+$ second-forbidden beta transition) and we assign an intensity of ≤11% to this branch.

A pair of less intense γ rays, with 2046 keV and 2349 keV, exactly match the energy difference between the 6^+, T=1 state and the lowest 4^+ state in ^{44}Ti. The 2046 keV γ ray, the stronger of the two, is coincident with the 1083 keV γ ray but not with any other one. Consequently, the 2046 keV γ ray cannot directly populate the 2454 keV, 4^+ state because then we would observe a γ2046- γ1371 coincidence as well (in addition to the observed γ2046 - γ1083 one). Thus, the 2046 keV γ ray must depopulate the 6849 keV state and be followed by the weaker 2349 keV γ ray, which populates the 2454 keV state. No coincidences with the 2349 keV γ ray are observed because we are not sensitive to coincidences with γ rays weaker than a few percent. The proposed decay route must proceed via a 4803 keV excited state in ^{44}Ti that has not been observed before. However, because the 2046 keV γ ray is more intense than the 2349 keV one, there must be another deexcitaton route from the 4803 keV state. This route must ultimately lead to the 1083 keV state (hence the observation of γ2046 - γ1083 coincidences) but is probably

fragmented so that each γ-ray path is below our detection limit. These routes are symbolically represented by the dashed lines in Fig. 2.

The decays of ^{44}V and ^{44m}V both funnel mainly through the lowest 2^+ state in ^{44}Ti, necessitating a separation of their contributions to the depopulation of this state. We postulate that 100% of the ^{44m}V decay is accounted for by the intensity of γ1371 plus that of γ2046 minus that of γ2349 (see Fig. 2). This result was subtracted from the total intensity of γ1083 and the remaining intensity was assigned to ^{44}V. We then postulate that 100% of the ^{44}V decay is accounted for by this remaining γ1083 intensity plus that of γ2531. The subsequently deduced intensities of γ rays assigned to ^{44}V and ^{44m}V are given in Table 1.

The proposed decay scheme for ^{44}V is shown in Fig. 2 and the intensities of its beta branches appear in Table 2. Three of the beta transitions are of an allowed character and one is superallowed. The presence of a superallowed branch to the known 2^+ state at 6606 keV in ^{49}Ti indicates a 2^+ assignment for ^{44}V and confirms the previous T=1 assignment to that state. The energies deduced for excited states in ^{44}Ti from our data agree well with the literature[15] and we have significantly reduced the energy uncertainty of the isobaric analogue state.

The lowest 6^+:T=1 state appears 242 keV above the lowest 2^+:T=1 state in ^{44}Ti (see Table 2) thus indicating a similar order in ^{44}V (and agreeing with that already known in the mirror, ^{44}Sc[15]) with the 6^+ state being the isomer and the 2^+ state being the ground state. In Fig. 2 we have placed the weak beta-delayed-alpha group seen by Cerny *et al.*[2] in the decay scheme for ^{44}V. Their measured half-life, 90±25 ms agrees with our

value for ^{44}V, 111±7 ms, but not for ^{44m}V, 150±3 ms. The centrifugal barrier for a low energy alpha group from an excited state in ^{44}Ti to ^{40}Ca (0^+) is significantly smaller for a 2^+ state than a 6^+ state, further supporting a ^{44}V assignment for this decay mode.

3.2 ^{52}Co

Two γ-ray spectra, obtained in our studies of the decay of ^{52}Co are shown in Fig. 3. It is evident from Fig. 3a that the heavy-ion reaction used to produce ^{52}Co is not as specific as the light-ion reaction used for the ^{44}V experiments (Fig. 1a). The γ rays attributed to ^{52}Co are much weaker than many other activities seen in Fig. 3a. Among the other activities produced, ^{42m}Sc, ^{50m}Mn, ^{52m}Mn and ^{52m}Fe originate from reactions of the ^{14}N beam with the Ca targets whereas ^{20}F, ^{24}Al and ^{28}P are produced from C and O contaminants on the target surfaces. The production rate of ^{52}Co was not large enough to permit an ISOL experiment. Consequently, assignment of γ rays to the decay of ^{52}Co must be based on known data[16] on levels in the beta-decay daughter ^{52}Fe.

The ^{52}Co nucleus is similar to ^{44}V in the sense that it consists of four holes in the $f_{7/2}$ shell whereas ^{44}V has four particles in that shell. Similar, closely spaced 2^+ and 6^+ isomers as seen for ^{44}V are thus expected for ^{52}Co and are known in its mirror nucleus, ^{52}Mn, where a 2^+ isomer is situated 378 keV above the 6^+ ground state[16]. The decay from ^{52}Co (6^+) should be very similar to that of ^{44m}V (6^+) (Fig. 2) with a strong 6^+:T=1 $\rightarrow 6^+ \rightarrow 4^+ \rightarrow 2^+ \rightarrow 0^+$ sequence in ^{52}Fe. The good agreement between the energies of four γ rays found in our work and the energy differences between the specified excited states in

^{52}Fe bears this out. The four γ rays listed in Table 3 were assigned to the decay of ^{52}Co on this basis.

The γ rays assigned to ^{52}Co exhibit the same apparent half-life and some are also found to be coincident (Table 3). These observations further support a ^{52}Co assignment. The half-life deduced for ^{52}Co from our data, 115±23 ms, does not agree with any other known activity in the vicinity of the compound nucleus. The unpublished half-life data of Miyatake *et al.*[6], 18±13 ms, does not agree with our value; however, their result was obtained with non-specific β counting and was presented with comments that it was unexpectedly short.

In Fig. 3a the 1942 keV γ ray assigned to ^{52}Co is not resolved from a 1944 keV γ ray from ^{50m}Mn. The centroid and intensity of the ^{52}Co portion of this doublet was deduced after the ^{50m}Mn portion had been subtracted, based on known, relative ^{50m}Mn γ-ray intensities[17]. Because of the increased uncertainty introduced by this procedure, and the low counting statistics, the 1942 keV peak could not be further decomposed for half-life analysis.

The γ-ray coincidence spectrum (Fig. 3b) shows the enhancement of ^{52}Co peaks, over the singles spectrum (Fig. 3a), when gates are set on the γ rays listed in Table 3. Gamma-ray peaks from some other intense activities are still seen in Fig. 3b as a result of γ-Compton and γ-β^+ coincidences in the 2 HPGe detectors as well as peaks from ^{50m}Mn originating from the gate on the 1942-1944 keV doublet.

Our proposed decay scheme for ^{52}Co is shown in Fig. 4. The excitation energies of states in ^{52}Co, deduced from our data, and shown in Table 4, are in good agreement with the data compiled by Junde[16]. The uncertainties have been reduced significantly.

Our deduced β feeding from ^{52}Co, shown in Table 4, clearly identifies the superallowed β transition to the IAS in ^{52}Fe. The determination of other possible β branches from ^{52}Co is more problematic for two reasons. The first is that our measured γ ray intensities imply β feeding to the 849 keV 2^+ state. Since this would require a highly forbidden β transition from ^{52}Co (6^+), it indicates the presence of the expected ^{52}Co (2^+) isomer in our data. Its decay should be similar to that of ^{44}V (Fig. 2), with the intensity split among several branches and the most intense γ ray ($2^+ \rightarrow 0^+$) being common with the decay of the 6^+ isomer. Thus, the specific signature of ^{52m}Co (2^+), namely a $2^+ \rightarrow 2^+$ γ ray at 1910 keV[16] (1448 keV for ^{44}V, see Table 1), should be weak, and even though this γ ray is absent in our spectra there still could be sufficient ^{52m}Co to explain the β feeding we observe to the 849 keV 2^+ state. We thus assume that this deduced β feeding, listed in brackets in table 4, arises from the decay of ^{52m}Co. Nevertheless, we have no specific evidence for this isomer. Because of the ambiguity of the origin of 849 keV γ rays their apparent half-life was not used for the ^{52}Co half-life determination in Table 3.

The other problem with the deduction of β branches from ^{52}Co is the intensity of the 1942 keV γ ray, which appears as a doublet with the 1944 keV γ ray from ^{50m}Mn. This γ ray intensity is required to establish the β branches to the 2385 and 4326 keV states and the uncertainties in the branches are therefore large. A slight change in the assumed doublet intensity separation produces large changes in the β branches. Because of these

two problems we have used 2σ uncertainties in evaluating the β feeding listed in the fourth column of Table 4. With these uncertainties, the feeding to the lowest 6^+ state is small or non-existent. This is in agreement with the predicted Gamow-Teller decay strengths shown in the next section.

4. THEORY AND COMPARISONS

The decay of ^{44}V is particularly interesting, as the full ($0\hbar\omega$) shell-model calculation is feasible and tests of truncation schemes within that model space can therefore be explored. In the heavier nucleus, ^{52}Co, full fp-shell calculations are not possible and the use of a truncation scheme is essential.

In the decay of ^{44}V (2^+), branches are observed to three 2^+, T=0 states and to the isobaric analogue state (IAS) 2^+, T=1 in the daughter nucleus, ^{44}Ti. A full fp-shell calculation for this decay has been given by Martinez-Pinedo and Poves[9] who used a slightly modified version of the Kuo-Brown[18] G-matrix (denoted by KB3 in ref.[19]) for the effective interaction, V. The results are given in the middle columns of Table 5. For the Gamow-Teller transition operator we use the standard one-body operator, $T= g_A \sigma \tau$, but use an in-medium value of the axial-vector coupling constant, g_A=1. For full ($0\hbar\omega$) shell-model calculations, it has been shown empirically in the sd-shell[20] and the pf-shell[21] that a value of g_A quenched from the free-nucleon value of 1.26 is required to fit measured beta-decay lifetimes. A theoretical interpretation involving configuration admixtures breaking the closed-shell cores (core polarization) and meson-exchange currents (including isobars) has been given by Arima *et al.*[22], and by Towner and

Khanna[23]. It is noted from Table 5 that the principal decay branches are reproduced and the computed lifetime agrees well with experiment. The calculation suggests about 10% of the decay branches go to states at higher excitation energy than the IAS, notably to the 1^+, T=1 and 3^+, T=1 states around 7.3 MeV. The main shortcoming of the calculation is that only two 2^+, T=0 states are produced at energies below the IAS compared to three observed in the beta-decay experiment and six listed in the nuclear data tables of Endt[15]. Weak-coupling model calculations suggest that these additional states are intruder states of configuration $(sd)^{-2}(pf)^6$.

The experimental data from the decay of ^{44m}V (6^+) together with results of a full fp-shell calculation are given in the middle columns of Table 6. Again, the calculation reproduces the main branches, predicts a lifetime in agreement with experiment, and suggests about 10% of the decays go to states at higher excitation energies than the IAS.

Next we consider a truncated model space in which only two of the fp-shell orbitals are active, namely the $f_{7/2}$ and $p_{3/2}$ orbitals, while the spin-orbit partner orbitals, $f_{5/2}$ and $p_{1/2}$, are excluded from the model space. What is required is a renormalized effective interaction, V^{eff}, operating in the truncated space that yields the same eigenvalues as the original interaction operating in the full fp-space. Bloch and Horowitz[24] have given a formal solution to this problem as a perturbation expansion in the original interaction, V:

$$V^{eff} = V + V\frac{Q}{\Delta E}V + \ldots . \qquad (1)$$

Here Q is a projection operator that restricts the intermediate states to being outside the truncated space, but still inside the full fp-shell space. Further, ΔE is the unperturbed energy difference between states inside and outside the truncated space which is expressed in terms of differences in single-particle energies of the orbitals involved. In evaluating ΔE we make the single-particle energies in the truncated space degenerate, $\mathcal{E}_{f7} = \mathcal{E}_{p3} = 0.0$ MeV, and likewise in the excluded space, $\mathcal{E}_{f5} = \mathcal{E}_{p1} = \Delta_p$, where Δ_p will typically be of the order of the spin-orbit splitting; namely 5 MeV. By making these single-particle energies degenerate we guarantee a Hermitian renormalized interaction, V^{eff}. Note that in second order, the interaction VQV produces both two-body and three-body operators. In our calculations we have neglected the three-body terms.

The one-body Gamow-Teller operator, T, must likewise be renormalized for use in a truncated model space. Again there is a perturbation expansion[25] in V which, through to second order, reads

$$T^{eff} = T + T\frac{Q}{\Delta E}V + V\frac{Q}{\Delta E}T$$

$$+ T\frac{Q}{\Delta E}V\frac{Q}{\Delta E}V + V\frac{Q}{\Delta E}T\frac{Q}{\Delta E}V + V\frac{Q}{\Delta E}V\frac{Q}{\Delta E}T$$

$$- VPV\frac{Q}{(\Delta E)^2}T - T\frac{Q}{(\Delta E)^2}VPV$$

$$-\frac{1}{2}V\frac{Q}{(\Delta E)^2}VPT - \frac{1}{2}TPV\frac{Q}{(\Delta E)^2}V, \qquad (2)$$

where P is a projection operator that restricts the intermediate states to being within the truncated space, P= 1-Q. Note that the first-order terms, TQV, lead to both one-body and two-body transition operators, while second-order terms such as TQVQV lead to one-body, two-body and three-body operators. Again we will neglect the three-body operators.

The results of these truncated-space calculations are given in the right-hand columns of Tables 5 and 6 where they can be compared with full fp-shell calculations. The agreement is very reasonable, suggesting that this procedure could be usefully implemented in heavier fp-shell nuclei. The Hamiltonian matrices for states involved in the beta decay of ^{44}V have dimensions of order 200 in the full fp-shell model space, compared to dimensions of order 20 in the truncated model space. Thus, there is a considerable reduction in the computational labour in preparing the Hamiltonian matrix. However, this is counterbalanced by the additional labour required in computing the two-body transition matrix elements involving the renormalized operator, T^{eff}, evaluated with truncated space eigenfunctions. Failure to use the complicated, renormalized operator can be crucial. For example, in the decay of the isomeric state, ^{44m}V(6^+), the calculated lifetime in the truncated model space is 126.4 ms with a bare one-body operator, T, and 151.8 ms with the renormalized operator, T^{eff}.

Next, we turn to the decay of ^{52}Co for which full fp-space calculation is not feasible. The dimensions of the Hamiltonian matrices for the 6^+ states in ^{52}Co and ^{52}Fe are

2.2 million for the T=0 state and 4.5 million for the T=1 state[26]. In the truncated space, with the further restriction that not more than two nucleons be placed in the $p_{3/2}$ orbital, the dimensions are of order 200. The role of the two-body renormalized transition operator is even more critical here because, in single-shell configurations, j^n, the expectation values of one-body operators are independent of n, while for two-body operators they scale as (n-1). Thus, as n goes from 4 at ^{44}V to 12 at ^{52}Co, the two-body operators become more important relative to the one-body operators. Let us illustrate this in an extreme case. Consider a model space comprising only one state, namely $f_{7/2}^n$ J=6 with lowest seniority, υ=2, and isospin T=1 for the parent state and T=0 for the daughter state in the beta decay of ^{44m}V (n=4) and ^{52}Co (n=12). The Gamow-Teller matrix element of T^{eff}, to first order in V, is given by

$$\langle T^{eff} \rangle = \alpha \langle f | T | f \rangle + (n-1)\beta \frac{\langle f^2 | V | fr \rangle}{E_f - E_r} \langle r | T | f \rangle$$

$$= \alpha \left\{ 1 + (n-1) \frac{\beta}{\alpha} \frac{\langle f^2 | V | fr \rangle}{E_f - E_r} \frac{\langle r | T | f \rangle}{\langle f | T | f \rangle} \right\} \langle f | T | f \rangle \qquad (3)$$

where f denotes the $f_{7/2}$ orbital and r denotes one of the excluded-space orbitals, in this case $f_{5/2}$. Here α and β are known quantities, given in terms of fractional-parentage coefficients and angular-momentum recoupling coefficients. The energy denominator, E_f-E_r, is simply the spin-orbit splitting between the $f_{7/2}$ and $f_{5/2}$ orbitals and is a negative quantity here. As a consequence, the second term in braces has opposite sign

to the leading term of unity. The cancellation between these two terms grows as n increases. Numerical values are given in Table 7. Note that to zeroth order, the Gamow-Teller matrix element is identical in ^{44m}V and ^{52}Co. This is just the particle-hole symmetry, the nucleus ^{44m}V being described by four particles in the $f_{7/2}$ shell and ^{52}Co by four holes in the same shell. This symmetry is broken by the renormalized operator. The two-body terms, as explained, grow rapidly with n such that in ^{52}Co the first-order corrections cancel a large fraction of the zeroth-order term. Because of this, the calculation is very sensitive to computational details. Note also that the second-order corrections are quite small compared to first order (although three-body terms have been neglected here), suggesting reasonable convergence by order.

Our results for the calculated lifetime and branching ratios for the beta decay of ^{52}Co are given in Table 8 for a bare Gamow-Teller transition operator, T, and for the renormalized operator, T^{eff}. The calculated branching ratio to the lowest 6^+, T=0 state in ^{52}Fe is very sensitive, as discussed earlier, to the role played by two-body operators, dropping by a factor of 4 in going from a bare to a renormalized operator; similarly, the total lifetime increases by a factor of 2. Thus, the decay data for ^{52}Co provide a very convincing demonstration of the need to use renormalized operators in truncated model spaces.

5. CONCLUSION

The beta decays of ^{44}V, ^{44m}V and ^{52}Co have been characterized for the first time. The superallowed β transitions have been identified and precise values for the excitation

energies of the isobaric analogue state in ^{44}Ti and ^{52}Co have been obtained. Other major β-decay branches were also observed. An isomeric state was found in ^{44}V and some evidence for one in ^{52}Co as well.

Shell-model calculations in the full fp-shell model space yield good agreement with the experimental data for ^{44}V and ^{44m}V. Calculations in a truncated space also yield good agreement with ^{44}V, ^{44m}V and ^{52}Co decay data and demonstrate the need for using renormalized operators in the truncated space. From the formal theory it is evident that the renormalized operators are dependent on the choice of model-space truncation. The same set of operators cannot be used for different truncations, a fact that is not universally recognized. The calculations in the full fp-shell model space also demonstrate that intruder configurations appear at low excitation energies even in such simple systems as ^{44}Ti.

REFERENCES

[1] T. Sekine, J. Cerny, R. Kirchner, O. Klepper, V.T. Koslowsky, A. Plochocki, E. Roeckl, D. Schardt, B. Sherill and B.A. Brown, Nucl. Phys. **A467** (1987) 93.

[2] J. Cerny, D.R. Goosman and D.E. Alburger, Phys. Lett. **37B** (1971) 380.

[3] E. Hagberg, V.T. Koslowsky, G. Savard and J.C. Hardy, Fall Meeting of the Division of Nuclear Physics of the APS, Bull. Am. Phys. Soc., **38** (1993) 1844, DD5., E. Hagberg, V.T. Koslowsky, G. Savard, J.C. Hardy and I.S. Towner, Nuclear Shapes and Nuclear Structure at low Excitation energies, Antibes, France, June 20-25, 1994, Edition Frontieres, p. 476, E. Hagberg, V.T. Koslowsky, G. Savard, J.C. Hardy and I.S. Towner, Exotic Nuclei and Atomic Masses 95, Arles, France, June 19-23, 1995, Edition Frontieres, p. 563.

[4] H. Keller, V. Borrel, D. Guillemaud-Mueller, A.C. Mueller, F. Pougheon, O. Sorlin, P. Baumann, F. Didierjean, A. Huck, A. Knipper, G. Walter, R. Anne, D. Bazin, M. Lewitowicz, M.G. Saint-Laurent and G. Marguier, Z. Phys. **A348** (1993) 67.

[5] F. Pougheon, J.C. Jacmart, E. Quiniou, R. Anne, D. Bazin, V. Borrel, J. Galin, D. Guerreau, D. Guillemaud-Mueller, A.C. Mueller, E. Roeckl, M.G. Saint-Laurent and C. Detraz, Z. Phys. **A327** (1987) 17.

[6] H. Miyatake, T. Shimoda, Y. Fujita, N. Takahashi, S. Morinobu and S. Hatori, Annual Report 1989, R.C. N.P. Osaka University, p. 72 (unpublished).

[7] M.J.G. Borge, P.G. Hansen, B. Jonson, S. Mattson, G. Nyman, A. Richter and K. Riisager, Z. Phys. **A332** (1989) 413.

[8] E.G. Adelberger, A. Garcia, P.V. Magnus and D.P. Wells, Phys. Rev. Lett. **67** (1991) 3658.

[9] G. Martinez-Pinedo and A. Poves, Phys. Rev. **C48** (1993) 937.

[10] E. Caurier, A.P. Zuker, A. Poves and G. Martinez-Pinedo, Phys. Rev. **C50** (1994) 225.

[11] E. Hagberg, T.K. Alexander, I. Neeson, V.T. Koslowsky, G.C. Ball, G.R. Dyck, J.S. Forster, J.C. Hardy, J.R. Leslie, H-B. Mak, H. Schmeing and I.S. Towner, Nucl. Phys. **A571** (1994) 555.

[12] H. Schmeing, J.C. Hardy, E. Hagberg, W.L. Perry, J.S. Wills, J. Camplan and B. Rosenbaum, Nucl. Instr. Meth. **186** (1981) 47.

[13] V.T. Koslowsky, M.J. Watson, E. Hagberg, J.C. Hardy, W.L. Perry, M.G. Steer, H. Schmeing, P.P. Unger and K.S. Sharma, Nucl. Instr. Meth. in Physics Research **B70** (1992) 245.

[14] J. Honkanen, V. Koponen, H. Hyvönen, P. Jaskinen, J. Äystö and K. Ogawa, Nucl. Phys. **A471** (1987) 489.

[15] P.M. Endt, Nucl. Phys. **A521** (1990) 750.

[16] H. Junde, Nuclear Data Sheets, **71** (1994) 659.

[17] T.M. Burrows, Nuclear Data Sheets **75** (1995) 1.

[18] T.T.S. Kuo and G.E. Brown, Nucl. Phys. **A114** (1974) 241.

[19] A. Poves and A.P. Zuker, Phys. Reports **70** (1981) 235.

[20] B.A. Brown and B.H. Wildenthal, At. Data Nucl. Data Tables, **33** (1985) 347.

[21] G. Martinez-Pinedo, A. Poves, E. Caurier and A.P. Zuker, Phys. Rev. **C53** (1996) 2602.

[22] A. Arima, K. Shimizu, W. Bentz and H. Hyuga, Adv. in Nucl. Phys., **18** (1987) 1.

[23] I.S. Towner, Phys. Reports, **155** (1987) 263; I.S. Towner and F.C. Khanna, Phys. Rev. Lett. **42** (1979) 51.

[24] C. Bloch and J. Horowitz, Nucl. Phys. **8** (1958) 91.

[25] I.S. Towner, *A Shell-Model Description of Light Nuclei* (Clarendon, Oxford, 1977) and references to the original literature cited there.

[26] T. Sebe and M. Harvey, *Enumeration of many body states of the Nuclear Shell Model with definite angular momentum and isobaric spin with mixed single-particle orbits*, Report AECL-3007, Chalk River Laboratories, 1968, unpublished.

TABLE 1

GAMMA RAYS ASSIGNED TO ^{44}V				
Eγ (keV)	**Iγ (%)**	**T½ (ms)**	**Visible In ISOL Exp.**	**Coincident Gamma Rays**
1083.08±0.10	90.8±10.5	140.3±3.7[a)]	yes	1448, (3032)
1447.88±0.13	21.7±2.2	100.2±10.6	yes	1083
2530.86±0.25	9.2±1.5	121.4±23.9		
2947.9±0.4[b)]	6.6±1.1	120.5±16.9[a)]		
3032.1±0.6	14.7±2.2	121.3±9.3		(1083)
4075.2±0.5	7.7±1.5	109.3±12.6		
5523.1±1.2	22.4±4.8	91.5±27.2		
	Average	111±7		
GAMMA RAYS ASSIGNED TO ^{44m}V				
Eγ (keV)	**Iγ (%)**	**T½ (ms)**	**Visible In ISOL Exp.**	**Coincident Gamma Rays**
1083.08±.10	100.0	140.3±3.7[a)]	yes	1371, 1561, 2046, 2833
1371.22±0.08	94.3±3.6	153.0±4.6	yes	1083, 1561, 2833
1561.00±0.08	85.9±3.5	149.0±4.0	yes	1083, 1371, 2833
2045.6±0.4	8.1±0.6	161.0±14.1		1083
2348.5±0.4	2.4±0.6	137.6±32.6		
2833.42±0.14	32.9±2.4	144.2±6.6	yes	1083, 1371, 1560
	Average	150±3		

a not included in T1/2 average
b tentative; not placed in level scheme

TABLE 2

LEVELS IN ^{44}Ti POPULATED IN THE DECAY OF ^{44}V				
Ex (keV)	**Ex[a] (keV)**	**J^{π}:T[a]**	**β Feeding (%)**	**Log ft.**
1083.09±0.10	1082.99±0.09	2^+	32±12	4.77
2530.97±0.14	2530.6±0.2	2^+	23.2±3.1	4.64
4115.3±0.6	4116.5±1.0	2^+	14.7±2.2	4.49
6606.4±0.5	6598±6	2^+:1	30.1±5.0	3.48
LEVELS IN ^{44}Ti POPULATED IN THE DECAY OF ^{44m}V				
Ex (keV)	**Ex[a] (keV)**	**J^{π}:T[a]**	**β Feeding (%)**	**Log ft.**
1083.09±0.10	1082.99±0.9	2^+	0	
2454.34±0.13	2454.33±0.15	4^+	≤11	
4015.37±0.15	4015.3±0.2	6^+	56.4±4.6	4.11
4803.05±0.35		$(4,5,6)^+$ [b]	0	
6848.84±0.22		6^+:1[b]	43.6±4.6	3.44

a from Ref. 15 except where noted
b assigned in this work

TABLE 3

GAMMA RAYS ASSIGNED TO ^{52}Co			
Eγ (keV)	**Iγ (%)**	**T½ (ms)**	**Coincident Gamma Rays**
849.43±0.10	100	104±11[a)]	1329, 1535, 1942 (3636)
1328.95±0.25	63±7	99±23	849
1535.27±0.15	69±6	149±33	849, 1942
1941.65±0.40	46±10	[b)]	849, 1535
	Average	115±23	

a not included in $T_{1/2}$ average
b overlaps with ^{50m}Mn γ ray. Not enough statistics for half-life deduction

TABLE 4

LEVELS IN ^{52}Fe POPULATED IN THE DECAY OF ^{52}Co				
Ex (keV)	**Ex[a)] (keV)**	**J^{π}:T[a)]**	**β Feeding (%)**	**Log ft.**
849.44±0.10	849.6±0.7	2^+	(31±14)[b)]	
2384.73±0.18	2385.7±1.0	4^+	<23	
4326.41±0.44	4329.7±2.3	$(6)^+$ [c)]	<24	
5655.37±0.51	5652±8	6^+:1	100	3.21

a from Ref. 16 except where noted
b see comments in text
c assigned in this work

TABLE 5

Branching ratios for allowed Gamow-Teller transitions in the beta decay of $^{44}V(2^+)$ from two theoretical calculations (see text) compared with experiment. Only states with theoretical branching ratios greater than 1% are tabulated.

Experiment			Theory-fp			Theory-f_7p_3		
$J^\pi;T$	Ex	BR%	$J^\pi;T$	Ex	BR%	$J^\pi;T$	Ex	BR%
$2^+;0$	1.08	32.0	$2^+;0$	2.33	42.6	$2^+;0$	2.74	51.6
$2^+;0$	2.53	23.2						
$2^+;0$	4.12	14.7	$2^+;0$	4.41	11.9	$2^+;0$	4.82	5.2
$2^+;1$	6.61	30.1	$2^+;1$	6.61	33.6	$2^+;1$	6.61	32.7
			$1^+;1$	7.31	5.6	$1^+;1$	7.32	4.8
			$3^+;1$	7.35	3.7	$3^+;1$	7.38	4.9
$t_{1/2}$(ms) = 111±7			$t_{1/2}$(ms) = 116.2			$t_{1/2}$ (ms) = 108.6		

TABLE 6

Branching ratios for allowed Gamow-Teller transitions in the beta decay of $^{44m}V(6^+)$ from two theoretical calculations compared with experiment. Only states with theoretical branching ratios greater than 1% are tabulated.

Experiment			Theo-fp			Theo-f_7p_3		
$J^\pi;T$	Ex	BR%	$J^\pi;T$	Ex	BR%	$J^\pi;T$	Ex	BR%
$6^+;0$	4.02	56.4	$6^+;0$	4.30	44.6	$6^+;0$	5.11	45.5
			$6^+;0$	6.53	0.1	$6^+;0$	6.86	2.6
$6^+;1$	6.85	43.6	$6^+;1$	6.85	40.3	$6^+;1$	6.85	42.5
			$5^+;0$	7.56	0.9	$5^+;0$	7.51	2.2
			$7^+;0$	7.56	1.0	$7^+;0$	7.82	1.2
			$7^+;1$	7.65	2.1	$7^+;1$	7.64	2.6
			$6^+;0$	7.76	7.0			
			$5^+;1$	8.13	2.5	$5^+;1$	8.14	1.7
$t_{1/2}$(ms) = 150±3			$t_{1/2}$(ms) = 149.2			$t_{1/2}$ (ms) = 151.8		

TABLE 7

The Gamow-Teller matrix element in the extreme limit of just one state in the truncated model space evaluated with the renormalized operator to zeroth-, first- and second-order in V.

	$\langle T^{eff} \rangle$			
	0^{th} order	**1^{st} order**	**2^{nd} order**	**Sum**
^{44m}V, n=4	1.195	-0.110	-0.008	1.077
^{52}Co, n=12	1.195	-0.737	0.030	0.488

TABLE 8

Branching ratios for allowed Gamow-Teller transitions in the beta decay of ^{52}Co in truncated f_7p_3 model space.

Experiment			**Theory (bare)**			**Theory (renorm)**		
$J^{\pi};T$	E_x	BR%	$J^{\pi};T$	E_x	BR%	$J^{\pi};T$	Ex	BR%
$6^+;0$	4.33	<24	$6^+;0$	4.75	33.7	$6^+;0$	4.75	8.9
			$6^+;0$	5.22	16.2	$6^+;0$	5.22	6.4
$6^+;1$	5.65	100	$6^+;1$	5.65	42.3	$6^+;1$	5.65	83.0
			$7^+;0$	6.34	3.2	$7^+;0$	6.34	0.9
			$7^+;1$	6.59	1.7	$7^+;1$	6.59	0.3
$t_{1/2}$(ms) = 115±23			$t_{1/2}$(ms) = 72			$t_{1/2}$ (ms) = 140		

FIGURE CAPTIONS

Fig. 1 Gamma-ray spectra obtained during our studies of ^{44}V. Panel (a) shows the beta-coincident spectrum obtained in the He-jet experiment (setup 1), (b) shows the equivalent spectrum obtained with the ISOL and (c) shows a coincidence spectrum obtained with a gate on the major ^{44}V 1083 keV γ ray (setup 2). Gamma-ray peaks are labeled with symbols either above or below the peaks and the symbols are explained in panels (a) and (b). Other unlabelled peaks originate from coincident summing or are single or double escape peaks.

Fig. 2 Proposed decay schemes for ^{44}V and ^{44m}V. The beta decay parent state has been aligned vertically with the isobaric analogue state in the daughter. The beta-delayed alpha branch shown for ^{44}V was not investigated in the present experiments but reported by Cerny et al.[2]. The dashed γ rays shown for ^{44m}V were not observed but represent one, or several, paths from the 4803 keV state to the 1083 keV state that must be present to explain our data (see text).

Fig. 3 Gamma-ray spectra obtained during our studies of the decay of ^{52}Co. Panel (a) shows the beta-coincident spectrum obtained in the He-jet experiment (setup 1) and (b) shows a coincidence spectrum (setup 2), which is the sum of four spectra produced with gates on the ^{52}Co γ rays, 849, 1329, 1535 and 1942 keV. Gamma-ray peaks are labeled with symbols either above or below the peaks and the symbols are explained in both

panels. Other unlabelled peaks originate from coincident summing or are single or double escape peaks.

Fig. 4 Proposed decay scheme for ^{52}Co. The beta-decay parent state has been aligned vertically with the isobaric-analogue state in the daughter.

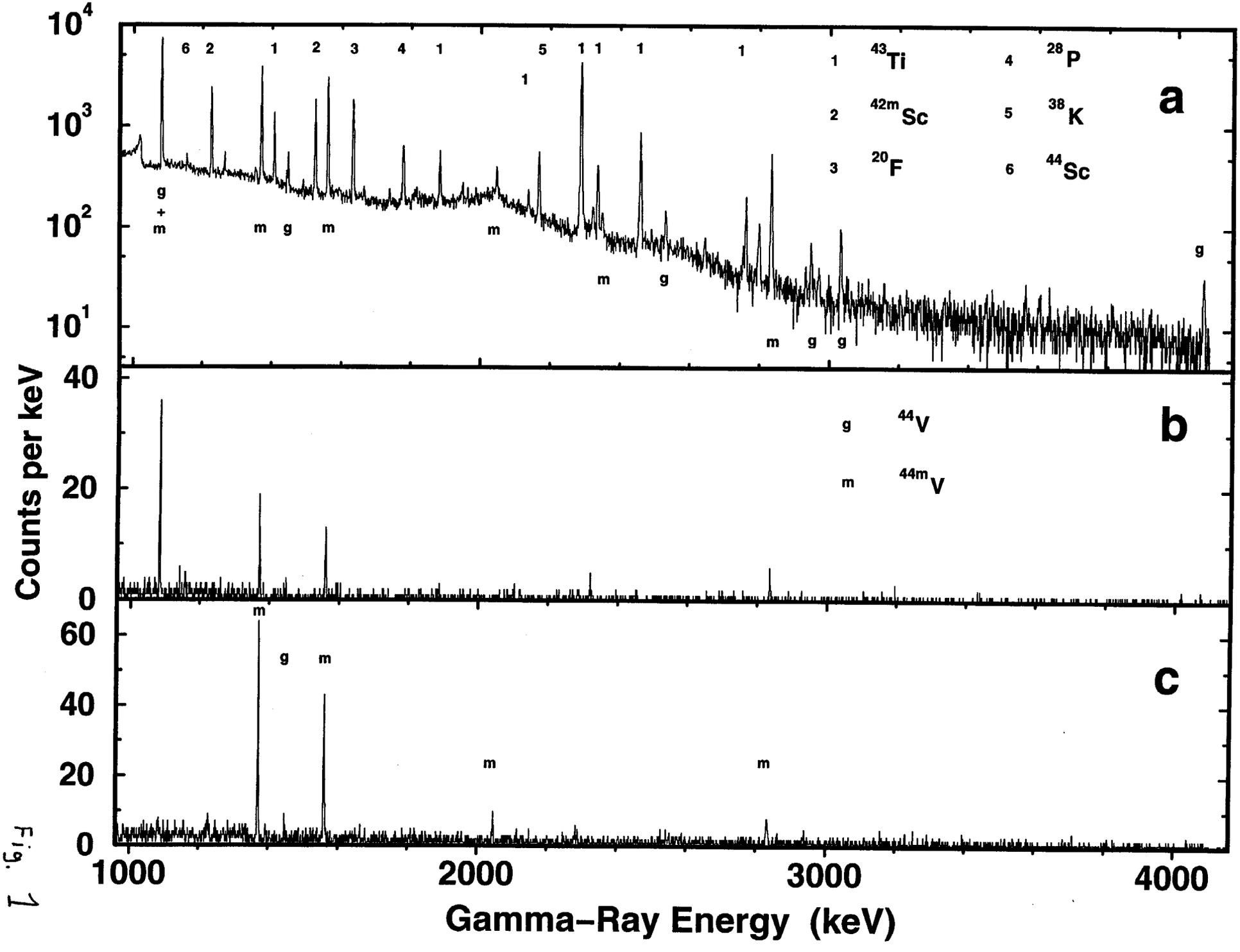
a
b
c
Counts per keV
Gamma–Ray Energy (keV)
1000
2000
3000
4000
10^4
10^3
10^2
10^1
40
20
0
60
40
20
0
1 ^{43}Ti
2 ^{42m}Sc
3 ^{20}F
4 ^{28}P
5 ^{38}K
6 ^{44}Sc
g ^{44}V
m ^{44m}V

Fig. 1

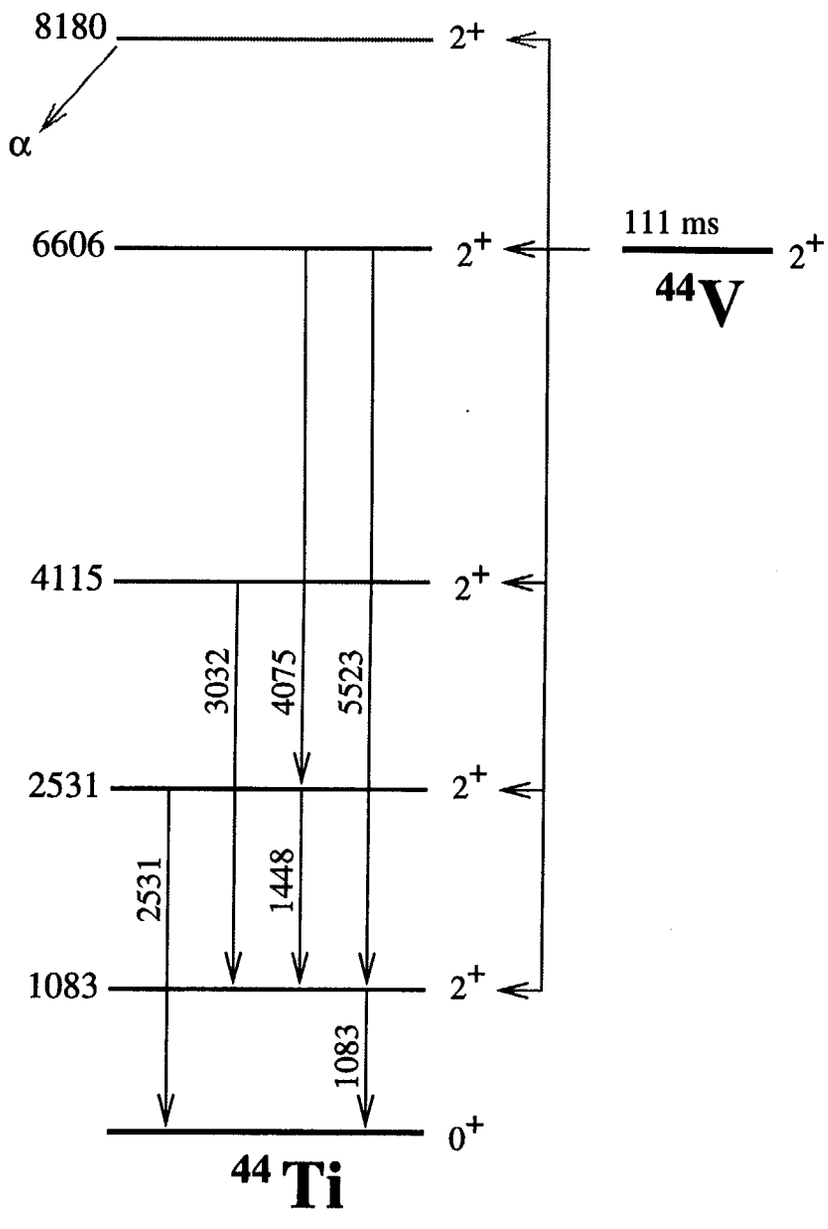
8180
2+
α
6606
2+
111 ms
2+
44V
4115
2+
3032
4075
5523
2531
2+
2531
1448
1083
2+
1083
0+
44 Ti

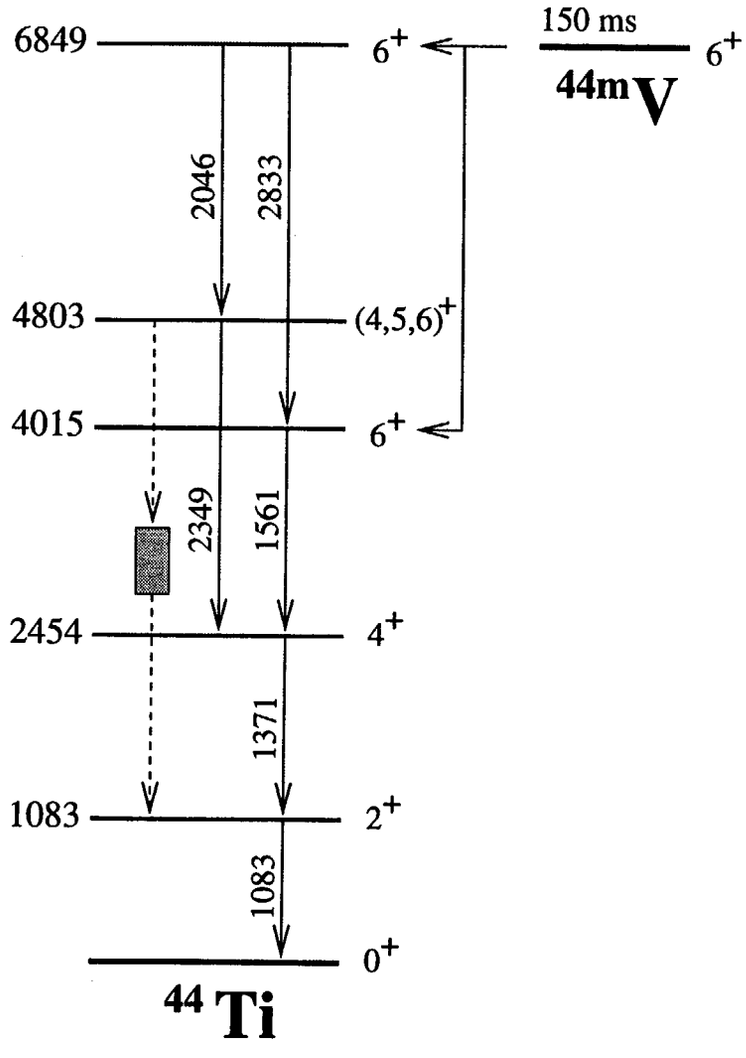
6849
6+
150 ms
6+
44mV
2046
2833
4803
(4,5,6)+
4015
6+
2349
1561
2454
4+
1371
1083
2+
1083
0+
44 Ti

Fig. 2

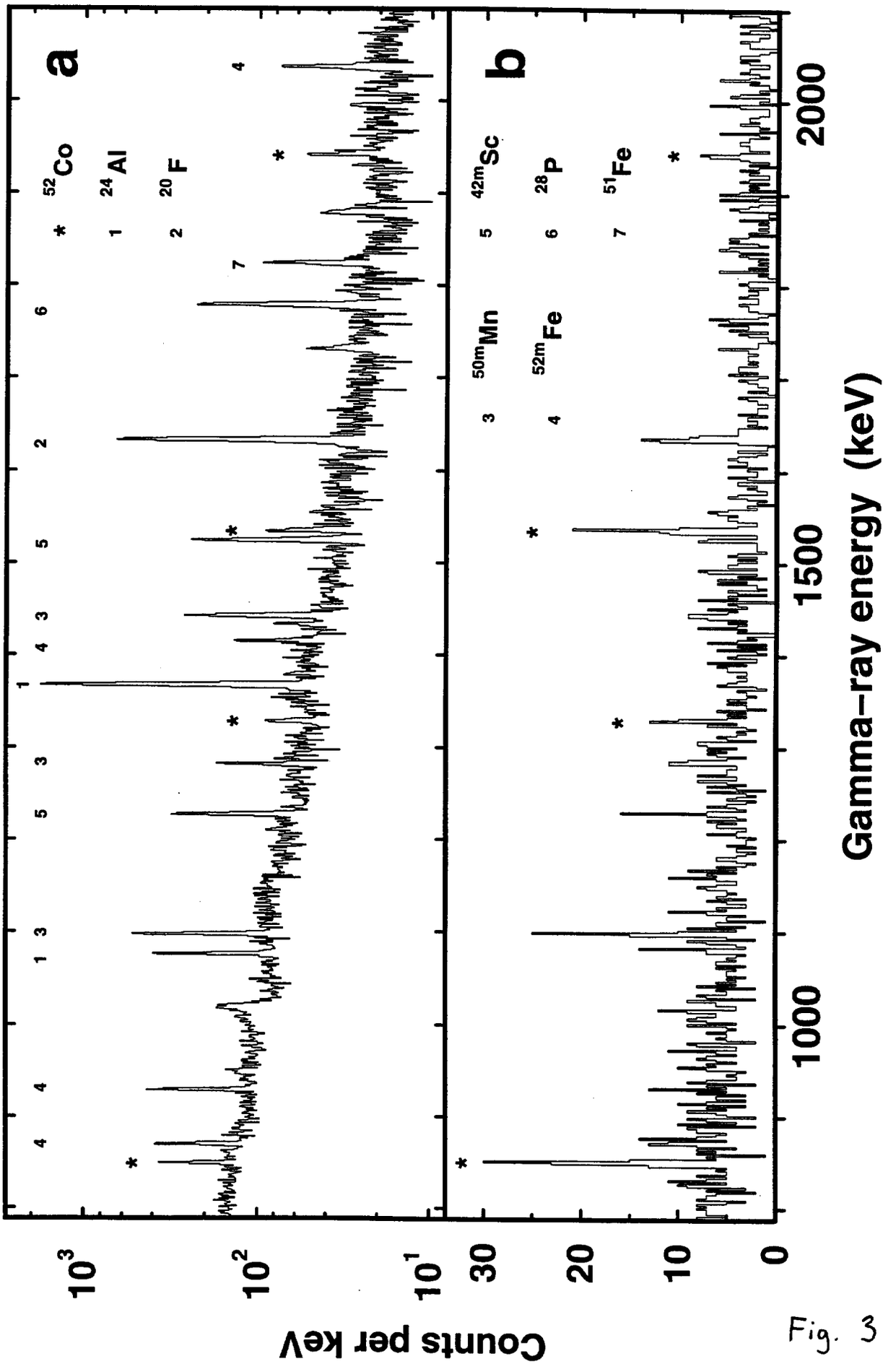
a
b
^{52}Co
^{24}Al
^{20}F
^{50m}Mn
^{52m}Fe
^{42m}Sc
^{28}P
^{51}Fe
Counts per keV
Gamma-ray energy (keV)

Fig. 3

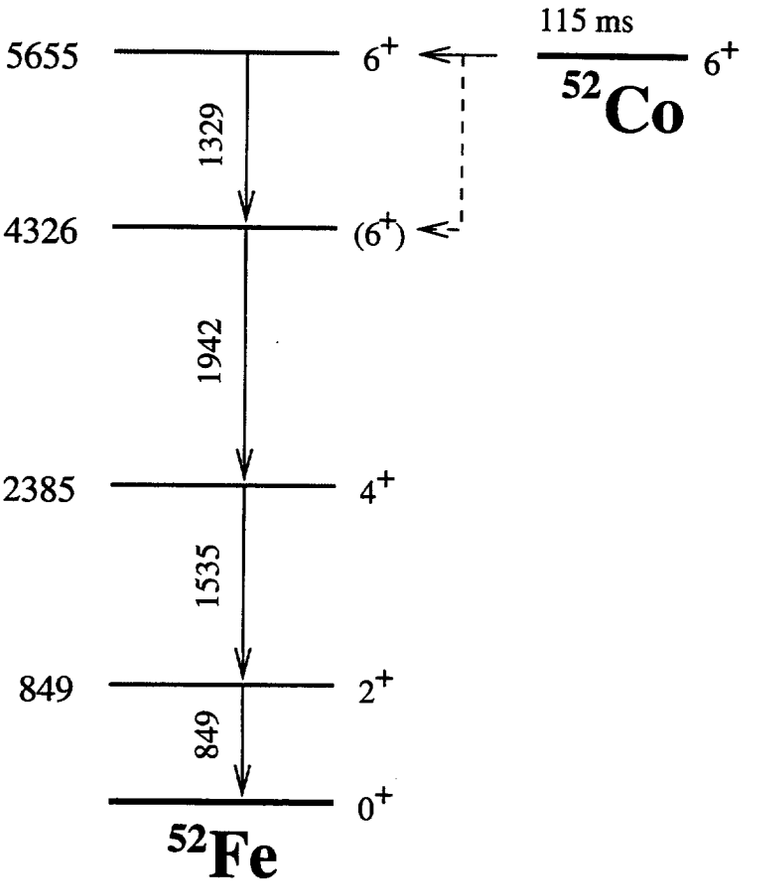

Fig. 4